NASA Technical Memorandum 88295

Accuracies of Southwell and Force/Stiffness Methods in the Prediction of Buckling Strength of Hypersonic Aircraft Wing Tubular Panels

William L. Ko

November 1987

National Aeronautics and
Space Administration

NASA Technical Memorandum 88295

Accuracies of Southwell and Force/Stiffness Methods in the Prediction of Buckling Strength of Hypersonic Aircraft Wing Tubular Panels

William L. Ko
Ames Research Center, Dryden Flight Research Facility, Edwards, California

1987

National Aeronautics and
Space Administration
Ames Research Center
Dryden Flight Research Facility
Edwards, California 93523-5000

SUMMARY

Accuracies of the Southwell method and the force/stiffness (F/S) method were examined when the methods were used in the predictions of buckling loads of hypersonic aircraft wing tubular panels, based on nondestructive buckling test data. Various factors affecting the accuracies of the two methods were discussed. Effects of load cutoff point in the nondestructive buckling tests on the accuracies of the two methods were discussed in great detail. For the tubular panels under pure compression, the F/S method was found to give more accurate buckling load predictions than the Southwell method, which excessively overpredicts the buckling load. It was found that the Southwell method required a higher load cutoff point, as compared with the F/S method. In using the F/S method for predicting the buckling load of tubular panels under pure compression, the load cutoff point of approximately 50 percent of the critical load could give reasonably accurate predictions.

INTRODUCTION

The accurate prediction of buckling loads of structural components, based on the nondestructive buckling test data, is generally a difficult problem. The graphical solution (buckling load prediction) is the test-data plotting schemes, test-data extrapolation schemes, and data fitting schemes. The well-known graphical method of predicting buckling loads is the Southwell method (or Southwell plot, refs. 1 to 5). In the Southwell plot, the compliance (that is, deflection/load) is plotted against deflection, and the buckling load is determined from the inverse slope of the plot. The Southwell method has been successful in predicting the classical buckling of simple structures such as columns and plates (see fig. 1, ref. 6). For complex structures exhibiting complex buckling behavior (for example, local instabilities and plasticity effect), the Southwell plot may not be a straight line, and therefore no discernable slope may be obtained for accurately determining the buckling loads (ref. 7).

The alternate method is the so-called force/stiffness (F/S) method proposed by Jones and Greene (ref. 8). In this method, the stiffness (such as force/normalized strain) is plotted against the force, and the buckling load is determined from the intersection of the limit strain line (the line with slope of unity in the F/S plot) and the extrapolation of the curve that fits the data points of the nondestructive buckling tests. This method eliminates the concerns about the linearity of the plot. The F/S method has been used extensively by Ko, Shideler, and Fields (ref. 9) and by Hedges and Greene (ref. 10) in the predictions of the buckling strength of hypersonic aircraft wing tubular and beaded panels under combined loadings. The F/S method seems to give satisfactory buckling load predictions, however, a critical review of the accuracy of this method is needed. This report presents the critical review of the accuracies of the Southwell method and the F/S method when they are applied to the predictions of buckling strength of hypersonic aircraft tubular panels (structures of complex geometry).

NOMENCLATURE

a	distance between two adjacent tubes, in
B_j	(j = 1, 2, 3) coefficients of second-order function for least-squares data fitting
C_i	(i = 1, 2, ..., 6) coefficients of third-order function for least-squares data fitting
CSG	capacitance strain gage
D	generalized strain variable
DT	displacement transducer
E	Young's modulus, lbf/in^2
F	applied load, lbf
F*	maximum applied load in nondestructive buckling tests, lbf
F/S	force/stiffness
f	width of panel flat region, in
k	extrapolation factor, F_{cr}/F^*
ℓ	length of tubular panel, in
m	exponent in the expression of D
N_x	panel compression load, lbf/in
N_{xy}	panel shear load, lbf/in
p	lateral pressure, lbf/in^2
R	radius of tubular wall, in
RSG	rosette strain gage
SG	axial strain gage
s	length of circular arc element of panel tube cross section
T	temperature, °F
t	thickness of tubular wall, in

$\bar{t}$	effective thickness of tubular panel, in
w	width of tubular panel, in
α	half angle of circular bead arc
ε_b	strain due to bending, in/in
ε_c	strain due to axial compression, in/in
γ	strain due to shear, in/in
δ	lateral displacement at center of tubular panel, in
$[\,]_{cr}$	critical value of [ ]

TUBULAR PANEL

Ko, Shideler, and Fields conducted extensive nondestructive buckling tests (ref. 9) of tubular panels made of two formed René 41 alloy sheets seam-welded together to form five flat regions (double sheets) and four noncircular tubular regions (fig. 1). At the end of these tests, panels 1 and 3 were loaded up to buckling failure under pure compression. Because the actual buckling loads of the tubular panel under pure compression are known, it is possible to examine the accuracy of the Southwell method and F/S method in predicting the buckling strength of the tubular panels under pure compression. The test data of panel 3 will be used in this accuracy study. Figure 2 shows the locations of the strain gages and the 11 lateral displacement transducers (DT) instrumented on panel 3 for pure compression tests, reported in reference 9. Figure 3 shows the buckled sites at the rear surfaces of tubes 1, 2, and 4 of test panel 3.

The data obtained from rosette strain gages RSG622, RSG623, and RSG633; axial strain gages SG516 and SG517; and the displacement transducer DT6 will be used in the study of accuracies of the aforementioned two methods of predicting buckling loads. That instrumentation was located in the center region of the panel and was relatively close to the buckled sites on tubes 1 and 2. Figure 4 shows the out-of-plane displacement of panel 3 at the time of buckling failure under pure compression (failure load F_{cr} = 41,051 lb, ref. 9). Notice that the deformation of the panel is a fundamental mode deformation with slight distortion near the buckled zone.

SOUTHWELL PLOT

The Southwell method has been successful in the prediction of classical buckling of simple structures such as columns and plates (refs. 1 to 5). For complex structures, such as a tubular panel with complex buckling behavior, the dependability of the Southwell method must be carefully examined. Using the results of the destructive buckling tests reported in reference 9, a Southwell plot was constructed for a tubular panel (panel 3), and is shown in figure 5. In the figure, F is the compressive load, and δ is the lateral displacement at the center of the panel.

It is seen that the data points lying in the region $0.43 < F/F_{cr} < 0.95$ (F_{cr} being the critical load at buckling) form a nice straight line. However, the inverse slope of this straight line yields the critical load of $F_{cr} = 55,184$ lb which is 34 percent higher than the actual buckling load of $F_{cr} = 41,051$ lb. Also, one notices that the data points lying within the region $0.96 < F/F_{cr} < 1.00$ form another straight line with a slightly steeper slope, yielding the critical load of $F_{cr} = 53,846$ lb. This value is approximately 31 percent over the prediction of the actual buckling load.

The second Southwell plot for tubular panel 3 shown in figure 6 is the plot of δ/N_x as a function of δ, where N_x is the effective panel compressive load calculated from the outputs of the two axial strain gages SG516 and SG517 located at the outer surfaces of tube 2 (see figs. 3, 7), namely:

$$N_x = \frac{E\bar{t}}{2} \left| \text{SG516} + \text{SG517} \right| \tag{1}$$

where E is the Young modulus and $\bar{t}$ (= 0.037 in) is the effective thickness of the tubular panel. Similar to figure 5, the data points in figure 6 also form a nice straight line in the region $0.43 < F/F_{cr} < 0.95$. The inverse slope of this straight line gives the critical panel load of $(N_x)_{cr} = 2687$ lb/in, which is 26 percent higher than the actual panel buckling load of $(N_x)_{cr} = 2138$ lb/in ($= F_{cr}/w = 41,051/19.2$), where w is the panel width (see fig. 1). Also, the data points lying in the region $0.96 < F/F_{cr} < 1.00$ form another straight line with a steeper slope, giving $(N_x)_{cr} = 2553$ lb/in, which is 19 percent above the measured value.

The final Southwell plot shown in figure 7 is the plot of δ/N_x as a function of δ, where the effective panel load N_x is calculated from the output of the rosette strain gage leg RSG622 located at the flat region of the center of the panel (see fig. 2), namely:

$$N_x = E\bar{t} \left| \text{RSG622} \right| \tag{2}$$

The plot, with the exception of a small strain region, is practically bilinear in shape. The inverse slope of the straight line fitting the data points lying in the region $0.43 < F/F_{cr} < 0.95$ gives the critical panel load of $(N_x)_{cr} = 2769$ lb/in, which is a 30 percent overprediction. The steeper straight line fitting the data points in the region $0.96 < F/F_{cr} < 1.00$ yield $(N_x)_{cr} = 2400$ lb/in gave a buckling load approximately 12 percent higher than the actual panel buckling load of $(N_x)_{cr} = 2138$ lb/in.

From the preceeding three Southwell plots for the tubular panel (see figs. 5 to 7), it is noticed that the plots are practically bilinear in shape (excluding the small strain region below $F/F_{cr} = 0.43$), and that the $F/F_{cr} = 0.95$ point lies almost at the middle of the plot. This means that the high loading data points in the region $0.95 < F/F_{cr} < 1.00$ spread over one-half span of the plot. Thus, in order to obtain the straight line zone for most accurately determining the slope, the nondestructive test has to be carried out up to 90 - 95 percent of the buckling load. For the case of the tubular panel, the Southwell method excessively overpredicts

the buckling load (either using the slope for the region $0.43 < F/F_{cr} < 0.95$, or for the region $0.96 < F/F_{cr} < 1.00$).

Figure 8 shows the Southwell plot for a square plate containing a central circular hole subjected to pure compression (ref. 7). For this plot, the ratio of hole diameter to plate length is 0.1. It is clear that the Southwell plot for this particular perforated plate is nonlinear, having no discernable slope for determining the buckling load.

During the nondestructive buckling tests, the Southwell plot may be displayed, say, on the screen of a cathode ray terminal (CRT) for observation of the growth of the plot. The test can be terminated if enough data points have formed a straight line. However, it is impossible to know the loading ratio F/F_{cr} of the test cutoff point because the location of the possible buckling point is unknown. As will be seen shortly, this problem does not occur in the F/S method.

FORCE/STIFFNESS METHOD

The force/stiffness (F/S) method, which is illustrated in figure 9, was developed by Jones and Greene (ref. 8) primarily for predicting the local buckling failure of complex structures (for example, beaded and tubular panels for hypersonic aircraft wings) under combined loading. The method was used extensively by Ko, Shideler, and Fields (ref. 9), and Hedges and Greene (ref. 10) in the nondestructive buckling strength predictions of beaded and tubular panels for a hypersonic aircraft wing. In this method, force F (which can be any particular load of applied load set) is plotted against stiffness F/D, where D is the generalized strain variable (refs. 9 to 10), and the buckling load is obtained at the intersection of the extrapolation of the curve fitting the nondestructive buckling test data points and the limit strain line (the line with slope of unity for which $D = D_{cr} = 1$, see fig. 9). The generalized strain variable D is defined as (ref. 8)

$$D = \frac{\varepsilon_c}{(\varepsilon_c)_{cr}} + \frac{\varepsilon_b}{(\varepsilon_b)_{cr}} + \left(\frac{\gamma}{\gamma_{cr}}\right)^m \tag{3}$$

where ε_c, ε_b, and γ are respectively the strains in compression, bending, and shear, $[\,]_{cr}$ denotes critical values, and the exponent m is an empirically determined constant. The values for ε_c, ε_b, and γ are obtained from the outputs of strain gage measurements, and $(\varepsilon_c)_{cr}$, $(\varepsilon_b)_{cr}$, and γ_{cr} must be calculated analytically using the buckling equations pertaining to panel local geometry (for instance, circular cylindrical panel for the tubular panel, refs. 8 to 10). At the critical local buckling strain state, equation (3) is set to unity, namely:

$$D = D_{cr} = 1 \tag{4}$$

which represents a critical strain interaction surface, as shown in figure 10.

Figure 11 shows the F/S plot of the same set of pure compression-destructive buckling data used in the earlier Southwell plots (see figs. 5 to 7). Unlike the Southwell plots, the data point of $F/F_{cr} = 0.95$ falls very close to the limit strain

line (D_{cr} = 1) since the abscissa is F instead of δ. This means that when the F/S method is used, the nondestructive buckling test can be cut off at a relatively lower loading level compared with the Southwell method (see fig. 5). The fact that the actual buckling point is very near the limit strain line implies the accuracy of the F/S plot. Notice that the data points in the region $0.3 < F/F_{cr} < 0.95$ form a smooth curve, and the curve that fits those data points intersects with the limit strain line at a point yielding a predicted buckling load almost equal to the actual buckling load.

Figure 12 shows the F/S plot (taken from ref. 9) for combined compression and shear loading $N_{xy}/N_x = 1.22$. When there is no lateral pressure acting, the F/S plot, except for the small load region, is usually strongly convex downward, allowing the least-squares data fitting to give relatively accurate predictions of the buckling load. When there is lateral pressure in addition to the combined compression and shear loading, the F/S plot usually turns out to be convex upward. This is shown in figure 13 (taken from ref. 9), for which $N_{xy}/N_x = 3.21$ and $p = 0.75$ lb/in^2. For a plot shape, like the one shown in figure 13, sometimes more accurate buckling load prediction could be obtained by curve-fitting only the higher load region and ignoring the lower load region, which is less important.

Accuracy of Force/Stiffness Method

The accuracy of the force/stiffness (F/S) method depends mainly on the following factors:

Test cutoff point. – The higher the load at which the nondestructive buckling test is cut off, the better the prediction of buckling load because the range of extrapolation of the data-fitting curve is shorter (or lower extrapolation factor $k = F_{cr}/F^*$, see fig. 9).

Mathematical function used in curve fitting. – The predicted buckling load will vary with the mathematical function chosen for the least-squares fitting of the data points. For combined compression, shear and lateral pressure loading, the F/S plot is always convex upward (see fig. 13). The least-squares fitting curve, based on a certain mathematical function, may tend to bend upward outside the data point range and may cause overprediction of the buckling load, or may not intersect with the limit strain line.

Range of curve fitting. – The data points in the lower load region are less important than the data points in the higher load region. The accuracy of the buckling load prediction could sometimes be improved by curve-fitting only the data points in the higher load region and ignoring the data points in the lower load region.

Exponent m. – The value of the exponent m in the expression of D will affect the value of D. The value of m for most types of panels was found to be nearly 2 (ref. 10). Thus, the effect of m on D is minimal.

Accuracy of $(\varepsilon_c)_{cr}$, $(\varepsilon_b)_{cr}$, γ_{cr}. – The value of D is affected by the accuracy of the calculated $(\varepsilon_c)_{cr}$, $(\varepsilon_b)_{cr}$, and γ_{cr}. Since the buckling theories used in the

calculations of $(\varepsilon_c)_{cr}$, $(\varepsilon_b)_{cr}$, and γ_{cr} are well established, the effect of the values of $(\varepsilon_c)_{cr}$, $(\varepsilon_b)_{cr}$, and γ_{cr} on the value of D or F/D could be very small.

Density of strain gage sites. – In using the F/S method, the test structure is instrumented with strain gages at different sites for monitoring local buckling. The greater the number of strain gage measurement sites, the better the chance to have some strain gage sites located near the potential buckle sites, and, therefore, a greater downward-bend region of the F/S plot may be obtained for more accurate prediction of the buckling load. Namely, the wider the downward-bend region is, the more accurately the data-fitting curve can give its extrapolation for determining the buckling load.

Test Cutoff Point

As previously mentioned, the most critical factor affecting the accuracy of the F/S plot is the location of the test cutoff point (for example, how far the test cutoff point is from the limit-strain line). The data presented in figure 11 may be used for the study of the effect of the location (or load level) of the test cutoff point on the accuracy of the F/S method. The load cutoff points selected for the preceding study were $F/F_{cr} = 0.5, 0.6, 0.7, 0.8, 0.9, 0.95$, and the following two types of mathematical functions were used in the least-squares data fittings:

1. Second-order function: $$\frac{F}{D} = B_1 + B_2F + B_3F^2 \tag{5}$$

2. Third-order function:

$$\frac{F}{D} = \frac{1 + C_1F + C_2F^2}{C_3 + C_4F + C_5F^2 + C_6F^3} \tag{6}$$

where B_j ($j = 1, 2, 3$) and C_i ($i = 1, 2, \ldots 6$) are constants determined from the least-squares fittings of the test data.

Figures 14 and 15 respectively show the F/S plots of test data of figure 11 fitted by the second-order and third-order functions up to different load cutoff points. In the least-squares data fittings, the insignificant data points in the region $F/F_{cr} < 0.3$ were neglected. The least-squares fitting for $F/F_{cr} = 0.8$ using the third-order function (equation (6)) gave poor extrapolation because the discontinuity (region of sudden slope change) fell near the force cutoff point $F/F_{cr} = 0.8$. For other values of F/F_{cr}, the discontinuity did not occur within the test data region $0.3 < F/F_{cr} < 1.0$, and therefore, it did not affect the buckling load predictions. The third-order function (equation (6)) was originally constructed for fitting the nondestructive buckling test data exhibiting sudden slope change (see figs. 9 and 12). For fitting the test data having a smooth slope change, equation (6) may not be ideal for certain values of F/F_{cr}. Overall it appears that the second-order function will give the most consistent prediction of buckling strength of tubular panels under pure compression. Table 1 summarizes different values of pure-compression buckling loads predicted from the plots in figures 14 and 15. The table also lists the error involved in each buckling load prediction. For the load cutoff points $F/F_{cr} = 0.5, 0.9, 0.95$, the third-order function gave more accurate

predictions. However in the region $0.6 < F/F_{cr} < 0.8$, the reverse is true. The data given in Table 1 suggest that when the F/S method is used in the prediction of buckling of tubular panels under pure compression, the nondestructive test may be terminated at a relatively low load cutoff point, say $F/F_{cr} = 0.5$.

CONCLUSIONS

Accuracies of the Southwell method and the F/S method were critically reviewed for the case when they were applied to the prediction of buckling loads of hypersonic aircraft wing tubular panels, based on the nondestructive buckling test data. Various factors that affect the accuracies of the two methods were discussed in great detail. For the case of tubular panels, the F/S method gave more accurate buckling load prediction than the Southwell method, which excessively overpredicts the buckling load. For pure compression, the F/S method could give reasonably accurate buckling load predictions, even with the load cutoff point as low as $F/F_{cr} \approx 0.5$. The Southwell method requires a much higher load cutoff point.

REFERENCES

1. Timoshenko, Stephen P.; and Gere, James M.: Theory of Elastic Stability. Mcgraw-Hill Book Co., N.Y., 1961, p. 191.

2. Spencer, H.H.; and Walker, A.C.: Critique of Southwell Plots with Proposals for Alternative Methods. Experimental Mechanics, vol. 15, August 1975.

3. Spencer, Herbert H.; and Walker, Alastair C.: Techniques for Measuring the Critical Loads of Columns and Plates. A Critical Review of Southwell Plots with Proposals for Alternative Methods. Society of Experimental Stress Analysis, Spring Meeting, Detroit, Michigan, March 14-17, 1974.

4. Cundari, F.L.; and Horton, W.H.: On the Applicability of the Southwell Plot to the Interpretation of Test Data from Instability Studies of Shell Bodies. American Inst. of Aeronautics and Astronautics, and American Society of Mechanical Engineers Structures, Structural Dynamics and Material Conference, 8th, Palm Springs, Calif., March 29-31, 1967, technical papers. New York, AIAA, Inc., 1967, p. 651-660.

5. Galletly, G.D.; and Reynolds, T.E.: A Simple Extension of Southwell's Method for Determining the Elastic General Instability Pressure of Ring Stiffened Cylinders Subject to External Pressure. SESA Proceedings, vol. XII, no. 2, 1955, p. 141.

6. Horton, W.H.; Cundari, F.L.; and Johnson, R.W.: The Analysis of Experimental Data Obtained from Stability Studies on Elastic Column and Plate Structures. Israel J. Tech., vol. 5, no. 1-2, 1967, pp. 104-112.

7. Schlack, Alois L., Jr.: Experimental Critical Loads for Perforated Square Plates. Proc. SESA, vol. 25, no. 1, Feb. 1968, pp. 69-74.

8. Jones, R.E.; and Greene, B.E.: The Force/Stiffness Technique for Nondestructive Buckling Testing. AIAA-74-351, April 17-19, 1974.

9. Ko, William L.; Shideler, John L.; and Fields, Roger A.: Buckling Behavior of René 41 Tubular Panels for a Hypersonic Aircraft Wing. AIAA-86-0978, May 19-21, 1986, (also published as NASA TM-86798, 1986).

10. Hedges, Phillip C.; and Greene, Bruce E.: Advanced Beaded and Tubular Structural Panels. NASA CR-132515.

TABLE 1. ACCURACIES OF BUCKLING LOADS IN PURE COMPRESSION PREDICTED FROM FORCE/STIFFNESS METHOD USING DIFFERENT LOAD CUTOFF POINTS AND LEAST-SQUARES DATA FITTING FUNCTIONS.

Load cutoff point F/F_{cr}	Predicted buckling load, F_{cr}, lb		Error, percent	
	Second-order function	Third-order function	Second-order function	Third-order function
0.5	43,350	39,770	5.60	3.12
0.6	44,660	45,840	8.79	11.67
0.7	42,930	45,430	4.58	10.67
0.8	42,690	46,110[a]	3.99	12.32[a]
0.9	42,160	40,580	2.70	1.15
0.95	41,950	41,170	2.19	0.29
1.0	41,051[b]	----	0	0

[a]Poor extrapolation curve.

[b]Actual buckling load.

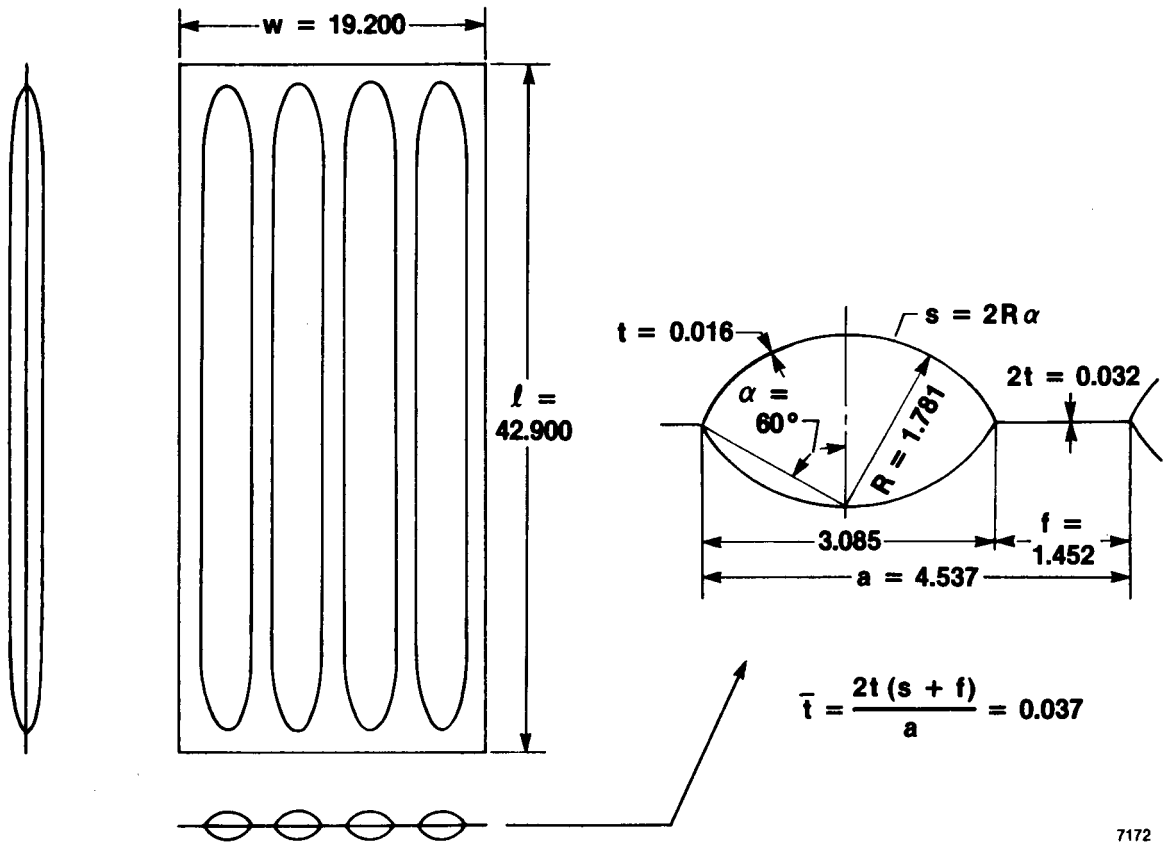

Figure 1. Geometry of tubular panel. Dimensions in inches.

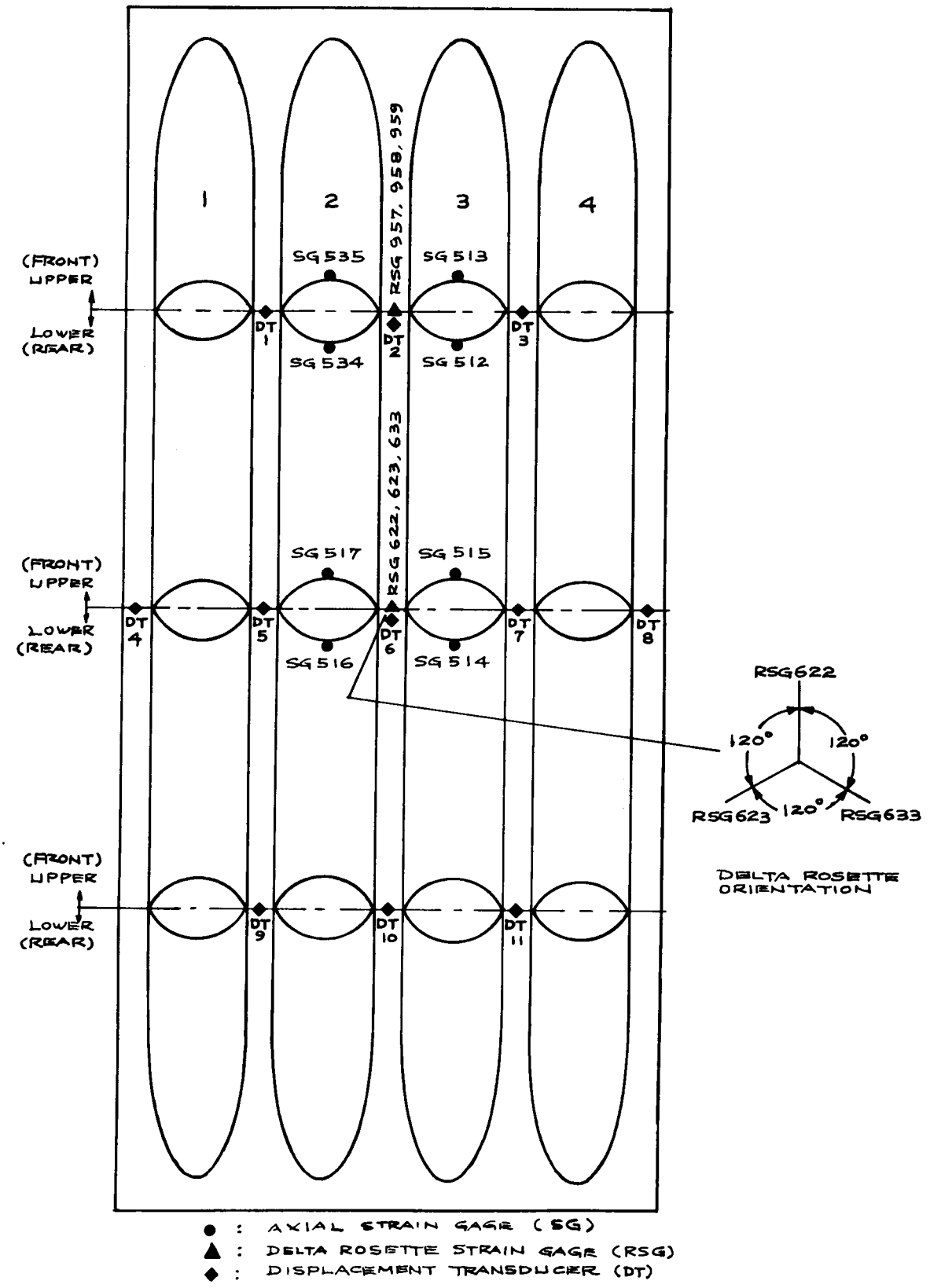

Figure 2. Instrumentation on test panel 3.

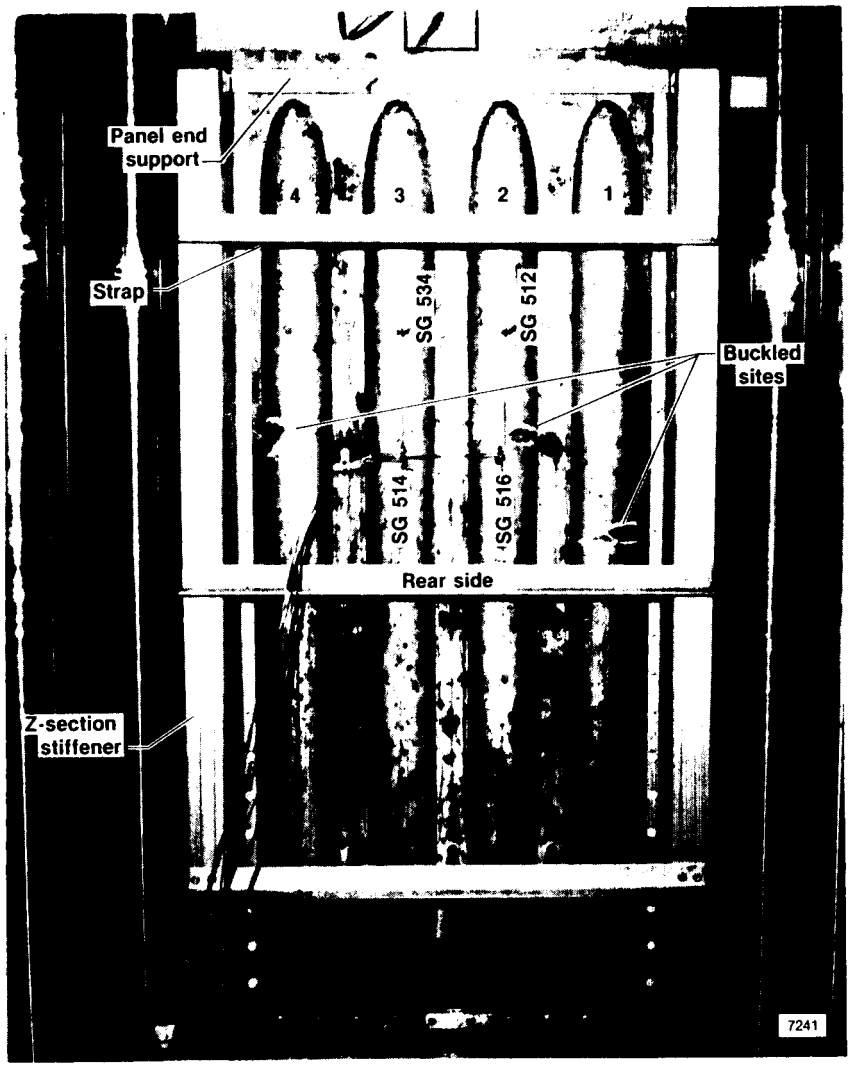

Figure 3. Buckled tubular panel 3, rear side, after pure compression test.

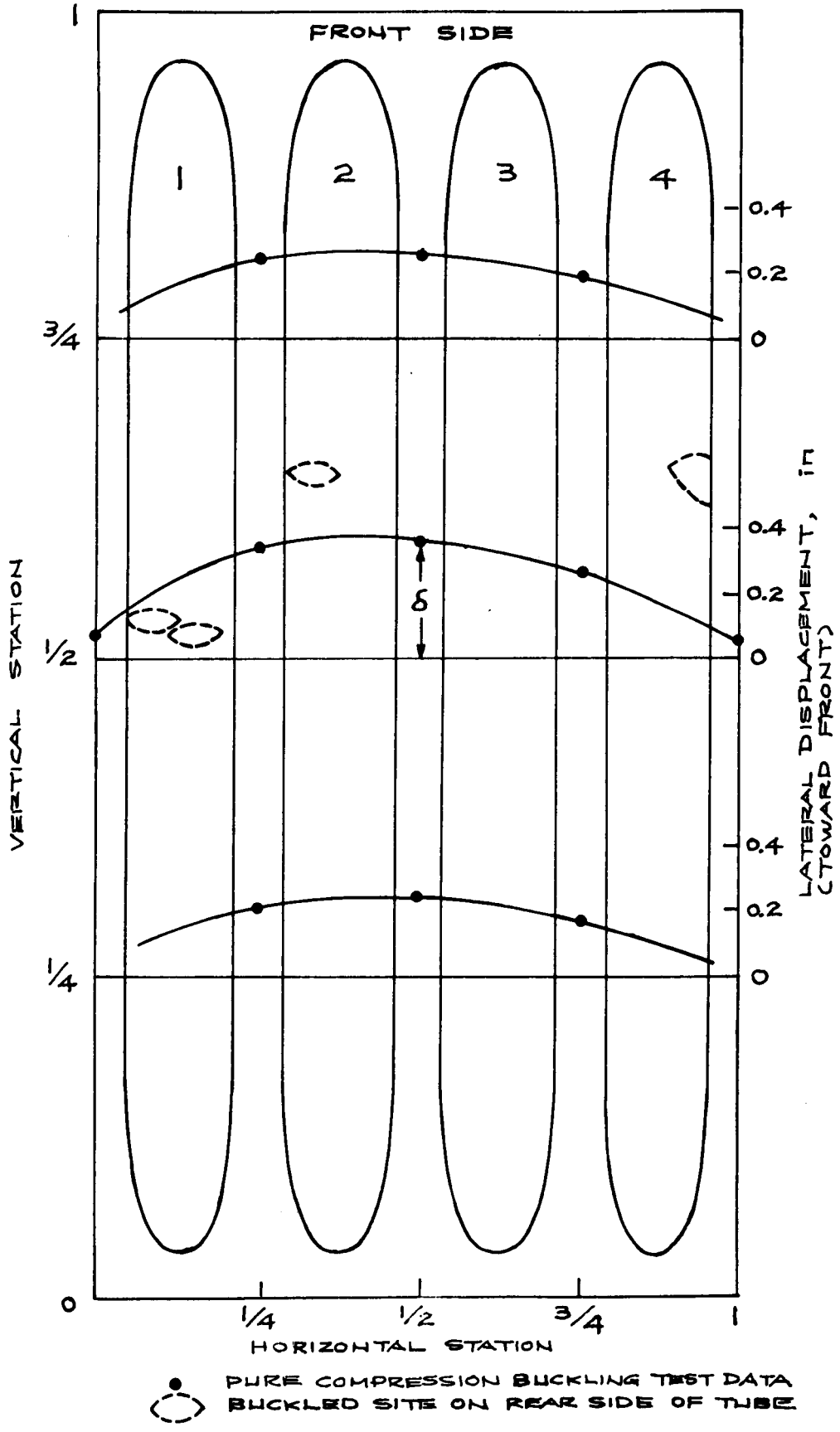

Figure 4. Out-of-plane deformation of test panel 3 at pure compression buckling. F_{cr} = 41,051 lb.

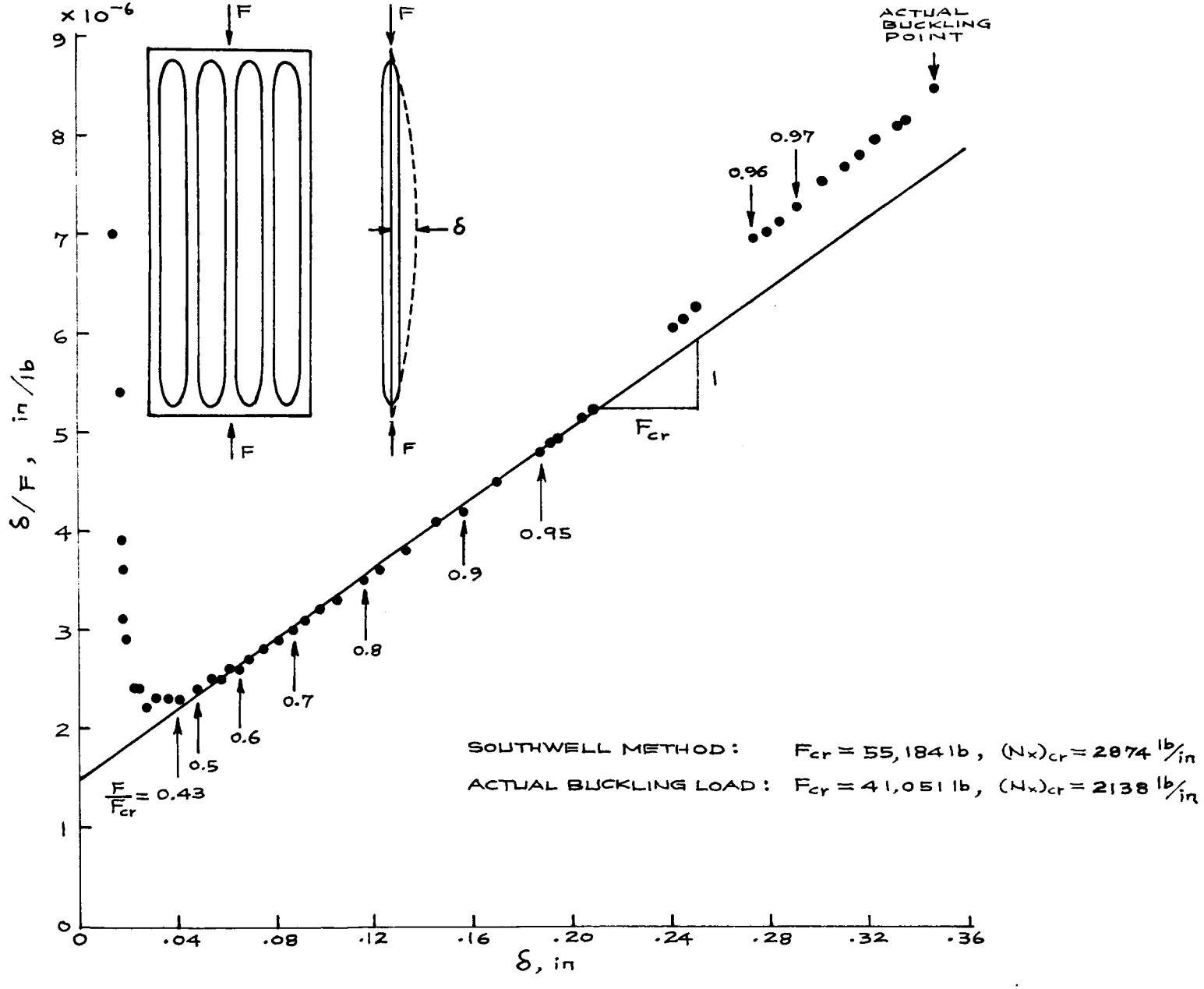

Figure 5. Southwell plot for tubular panel 3 under pure compression.

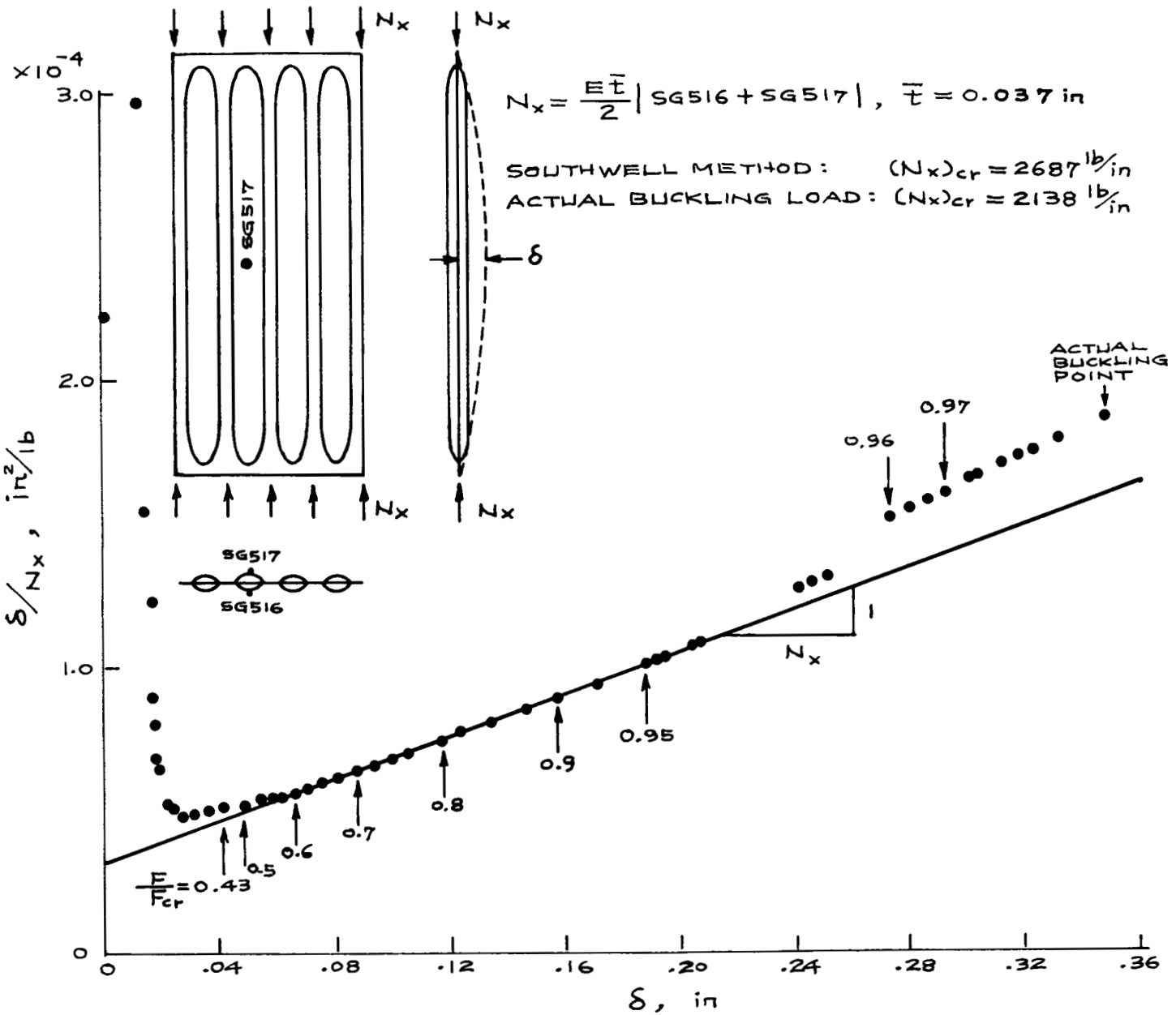

Figure 6. Southwell plot for tubular panel 3 under pure compression. N_x calculated from outputs of SG516 and SG517.

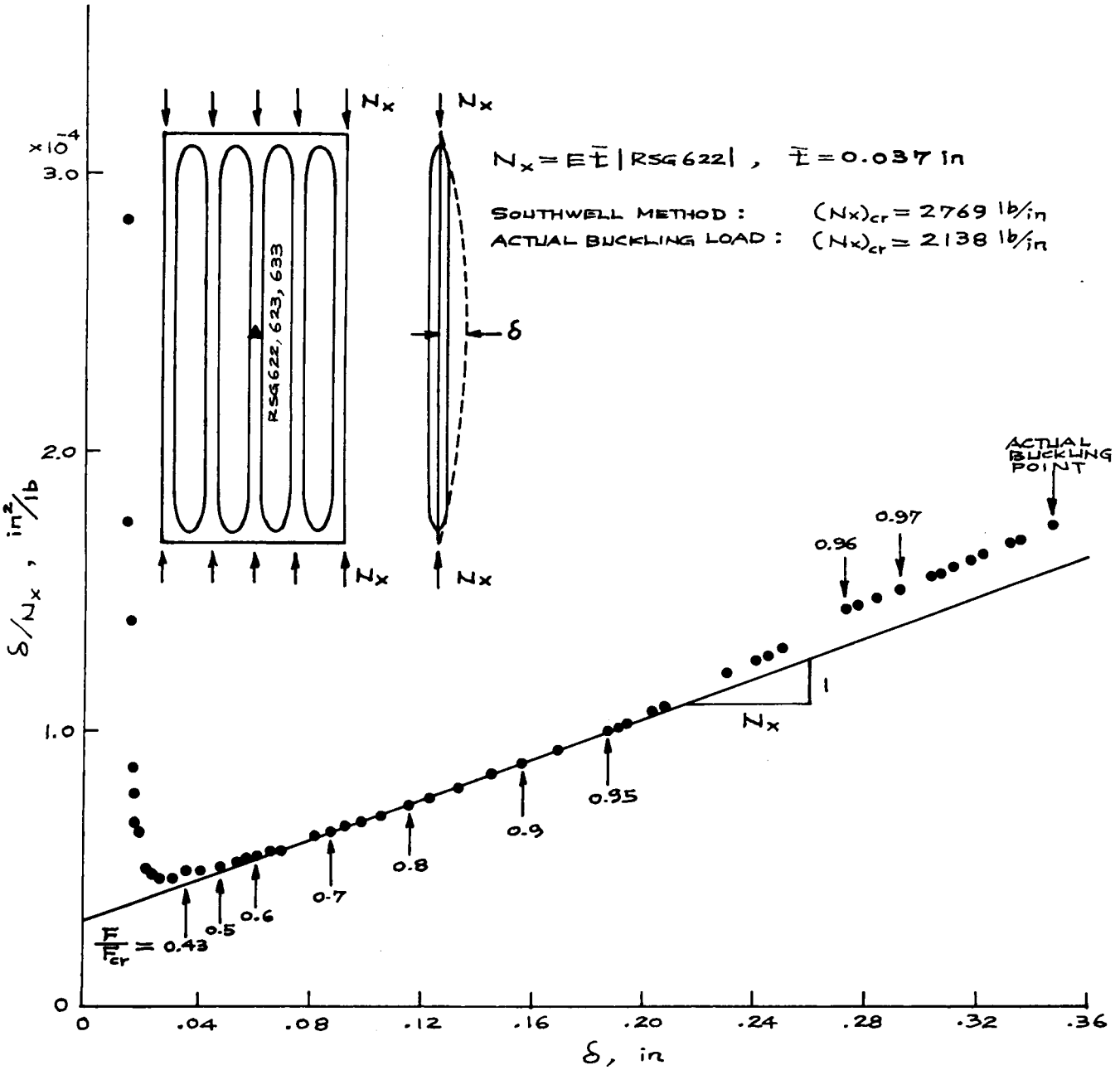

Figure 7. Southwell plot for tubular panel 3 under pure compression. N_x calculated from output of RSG622.

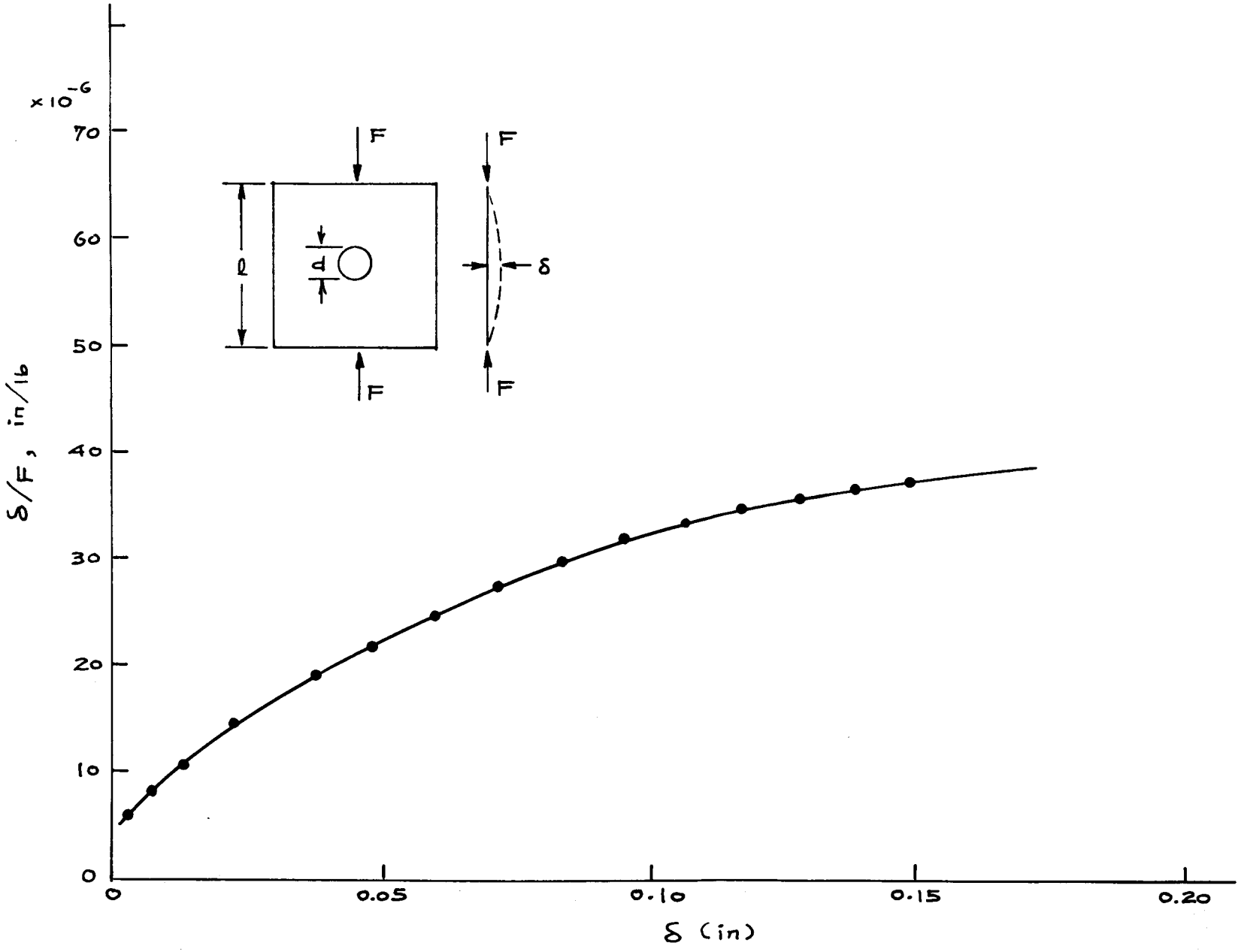

Figure 8. Southwell plot for a square plate containing a central circular hole under pure compression (ref. 7, for d/ℓ = 0.1).

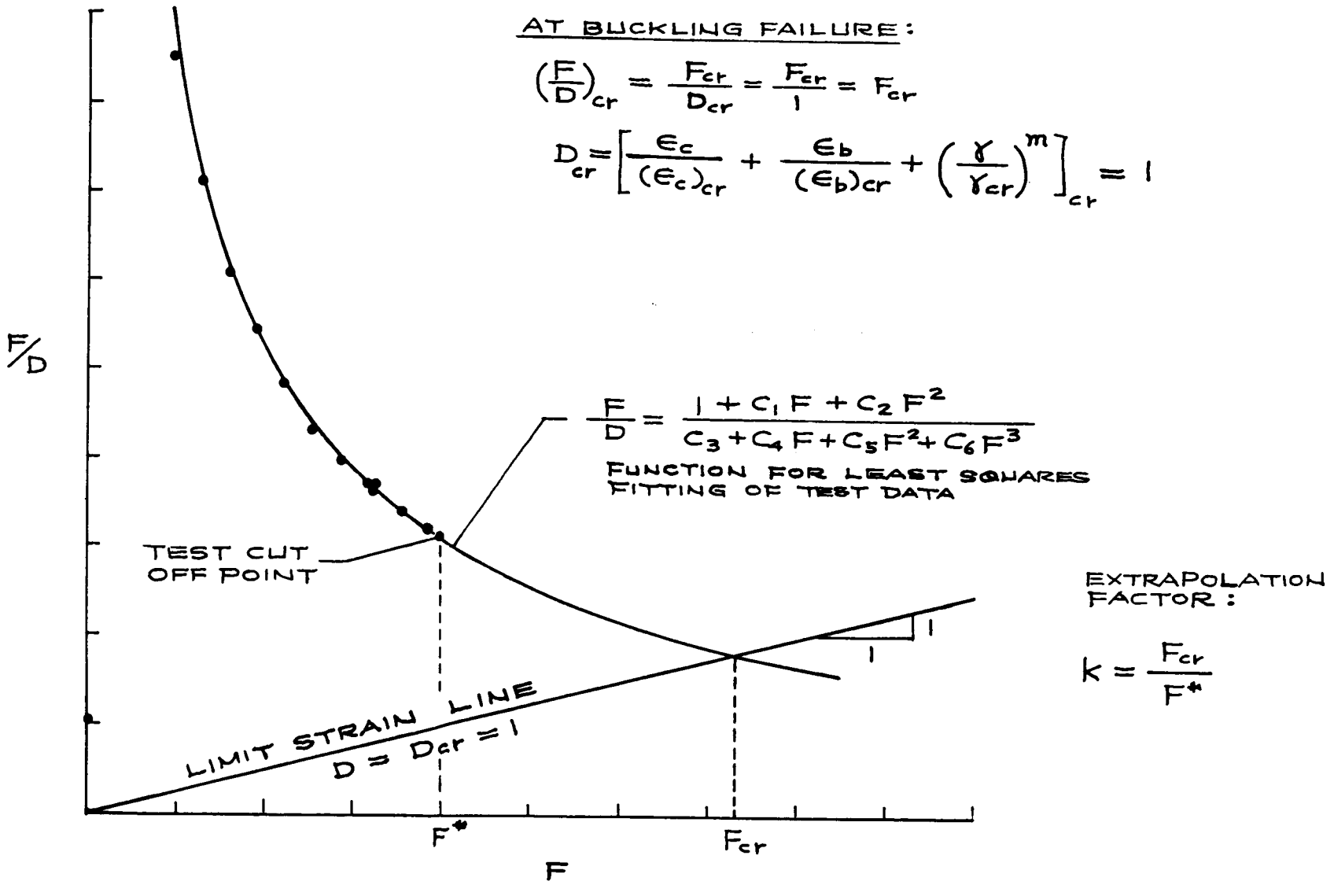

Figure 9. Force/stiffness plot for local buckling.

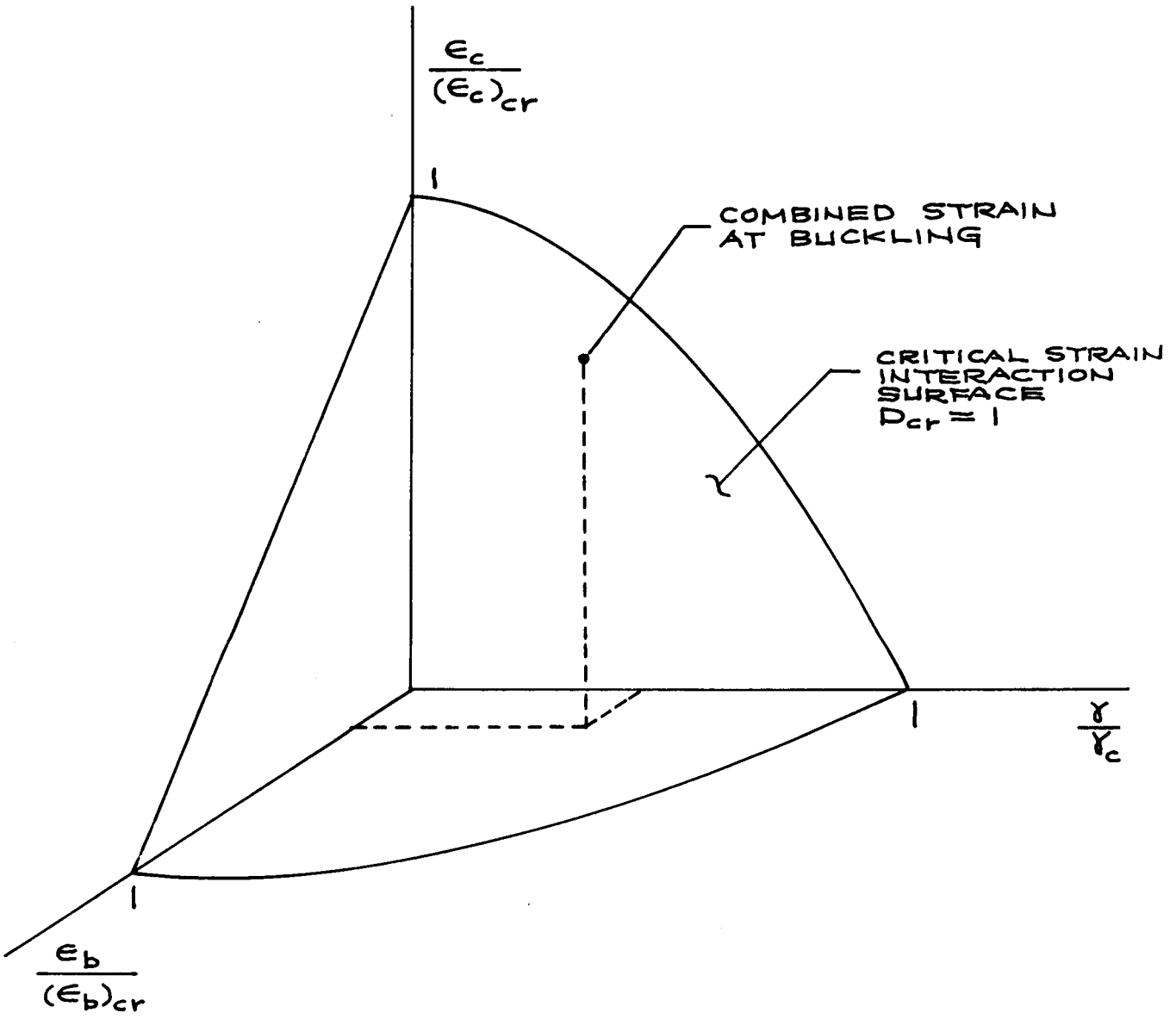

GENERALIZED STRAIN VARIABLE

$$D = \frac{\epsilon_c}{(\epsilon_c)_{cr}} + \frac{\epsilon_b}{(\epsilon_b)_{cr}} + \left(\frac{\gamma}{\gamma_c}\right)^m$$

CRITICAL STRAIN INTERACTION SURFACE

$$D = D_{cr} = 1$$

Figure 10. Critical strain interaction surface.

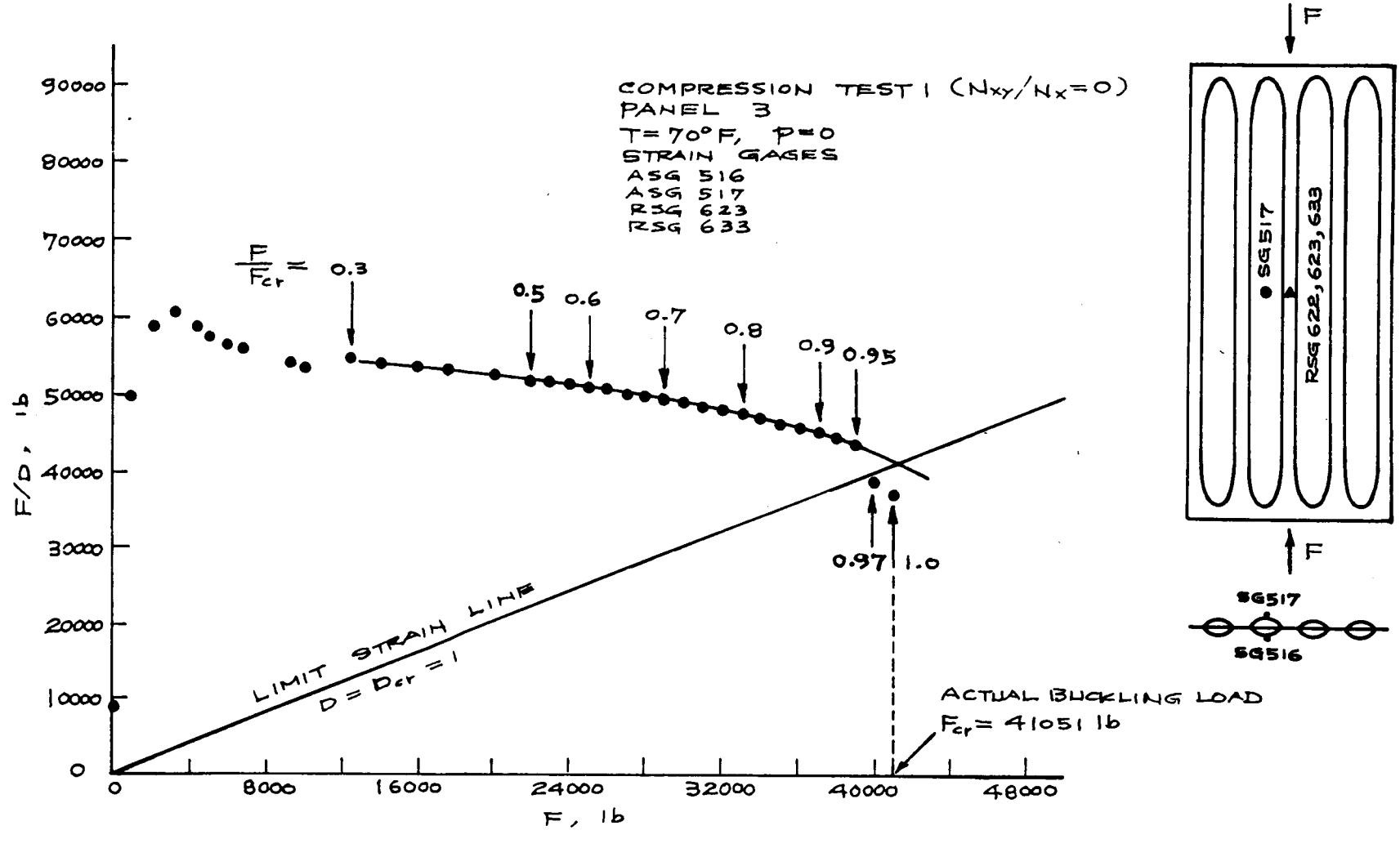

Figure 11. Force/stiffness plot for tubular panel 3 under pure compression.

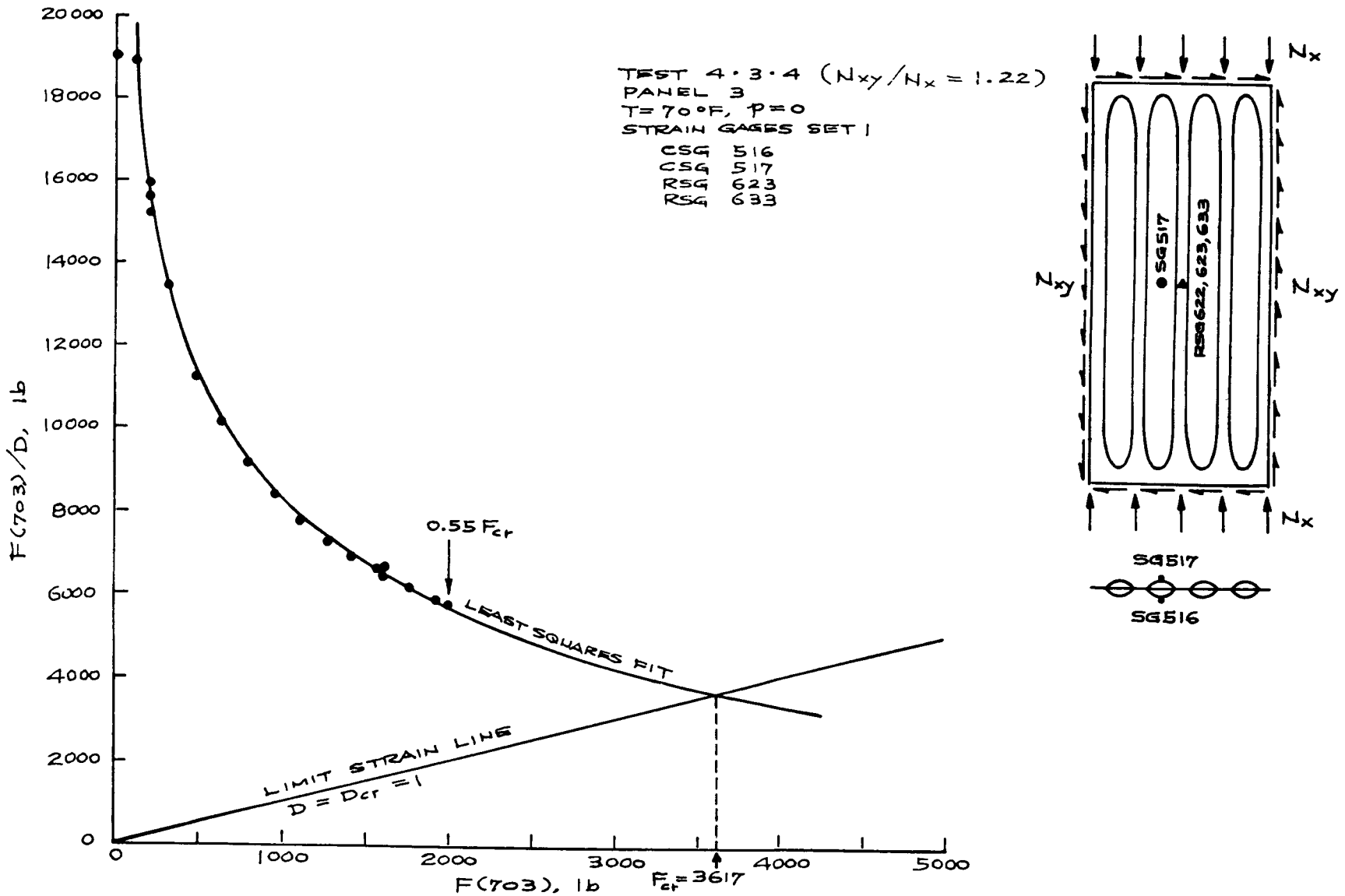

Figure 12. Force/stiffness plot for tubular panel 3 under combined loading (compression, shear). N_{xy}/N_x = 1.22.

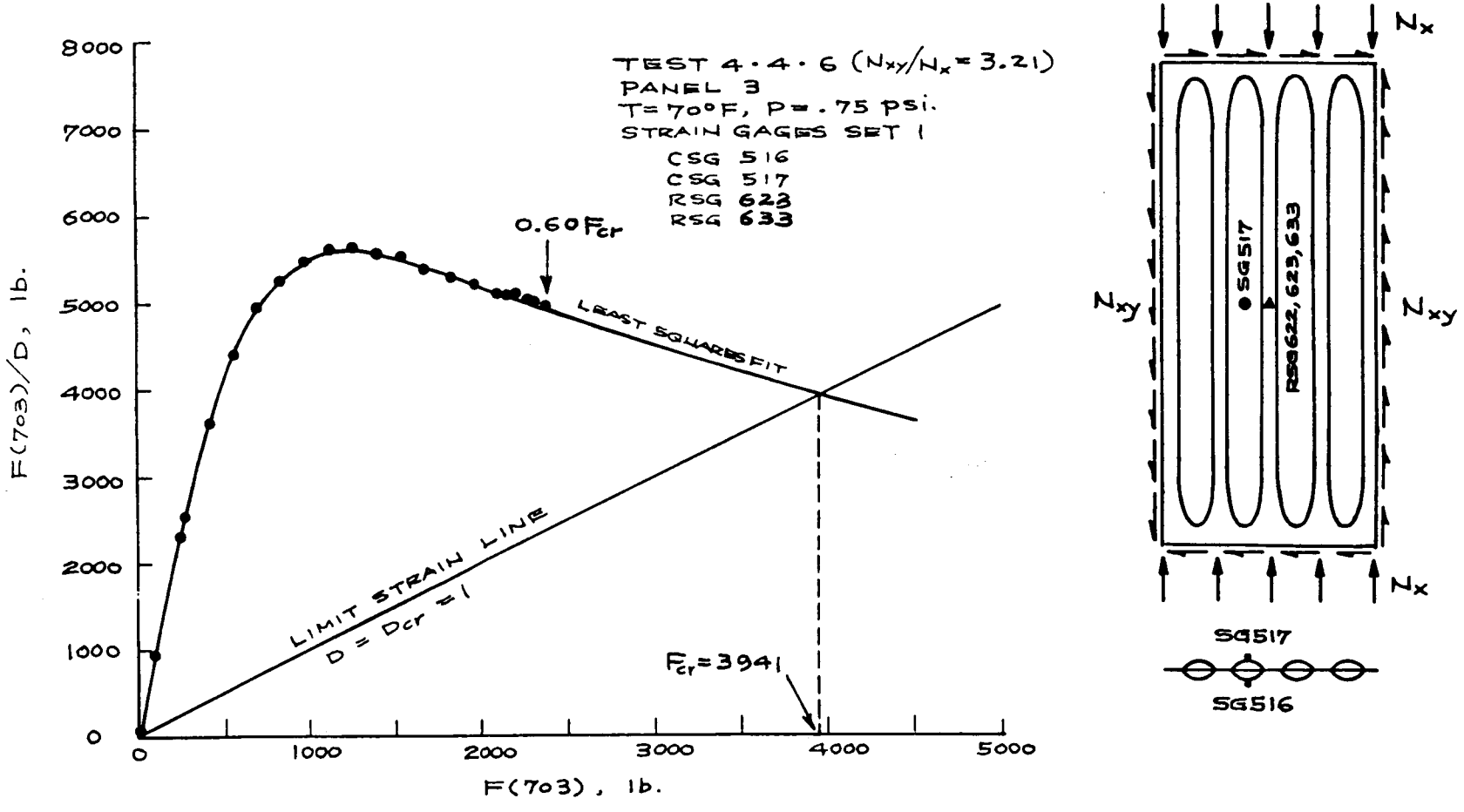

Figure 13. Force/stiffness plot for tubular panel 3 under combined loading (compression, shear, lateral pressure). N_{xy}/N_x = 3.21.

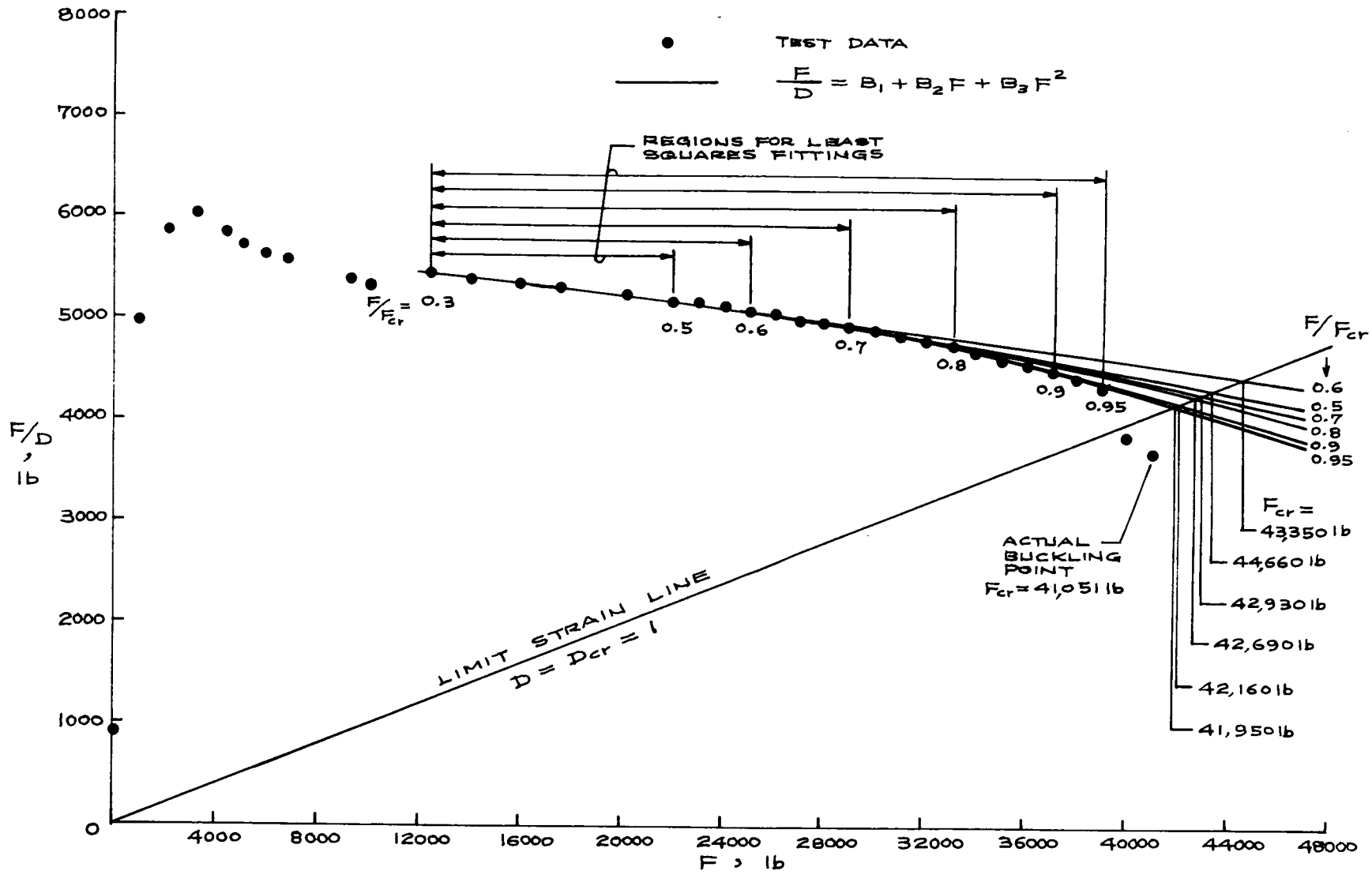

Figure 14. Least-squares fittings of different regions of pure compression buckling test data of tubular panel using second-order function.

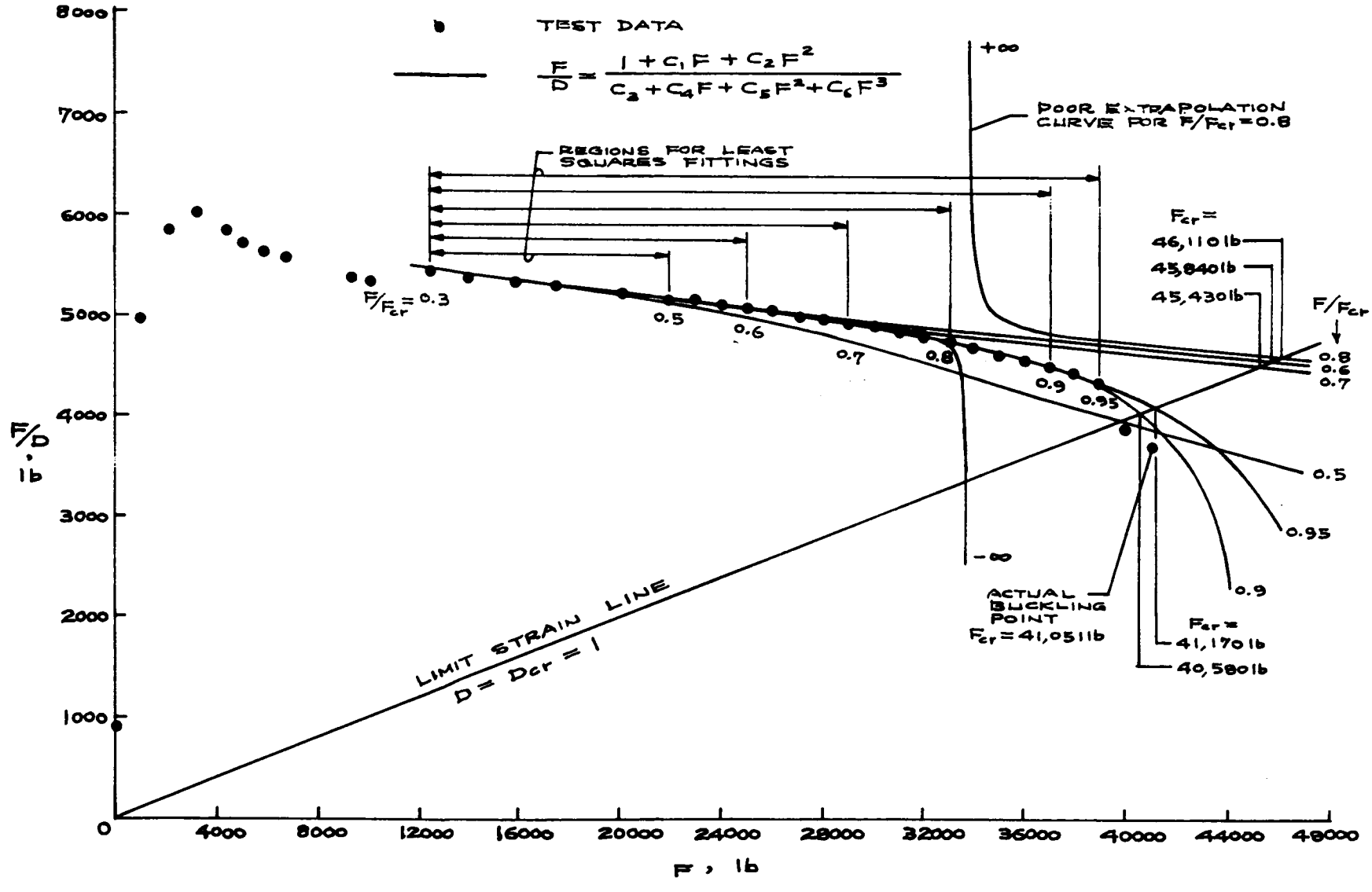

Figure 15. Least-squares fittings of different regions of pure compression buckling test data of tubular panel using third-order function.

1. Report No. NASA TM-88295	2. Government Accession No.	3. Recipient's Catalog No.
4. Title and Subtitle ACCURACIES OF SOUTHWELL AND FORCE/STIFFNESS METHODS IN THE PREDICTION OF BUCKLING STRENGTH OF HYPERSONIC AIRCRAFT WING TUBULAR PANELS		5. Report Date November 1987 6. Performing Organization Code
7. Author(s) William L. Ko		8. Performing Organization Report No. H-1415
9. Performing Organization Name and Address NASA Ames Research Center Dryden Flight Research Facility P.O. Box 273 Edwards, CA 93523-5000		10. Work Unit No. RTOP 506-53-51 11. Contract or Grant No.
12. Sponsoring Agency Name and Address National Aeronautics and Space Administration Washington, DC 20546		13. Type of Report and Period Covered Technical Memorandum 14. Sponsoring Agency Code

15. Supplementary Notes

16. Abstract

Accuracies of the Southwell method and the force/stiffness (F/S) method were examined when the methods were used in the predictions of buckling loads of hypersonic aircraft wing tubular panels, based on nondestructive buckling test data. Various factors affecting the accuracies of the two methods were discussed. Effects of load cutoff point in the nondestructive buckling tests on the accuracies of the two methods were discussed in great detail. For the tubular panels under pure compression, the F/S method was found to give more accurate buckling load predictions than the Southwell method, which excessively overpredicts the buckling load. It was found that the Southwell method required a higher load cutoff point, as compared with the F/S method. In using the F/S method for predicting the buckling load of tubular panels under pure compression, the load cutoff point of approximately 50 percent of the critical load could give reasonably accurate predictions.

17. Key Words (Suggested by Author(s))	18. Distribution Statement
Accuracy of buckling load predictions Force/stiffness method Southwell method Tubular panel	Unclassified – Unlimited Subject category 39

19. Security Classif. (of this report)	20. Security Classif. (of this page)	21. No. of Pages	22. Price*
Unclassified	Unclassified	26	A03

For sale by the National Technical Information Service, Springfield, Virginia 22161.